

---

# Tackling Unbounded State Spaces in Continuing Task Reinforcement Learning

---

Brahma S. Pavse<sup>1</sup>, Yudong Chen<sup>1</sup>, Qiaomin Xie<sup>2</sup>, Josiah P. Hanna<sup>1</sup>

<sup>1</sup>Department of Computer Science, University of Wisconsin – Madison

<sup>2</sup>Department of Industrial and Systems Engineering, University of Wisconsin – Madison

Corresponding author: pavse@wisc.edu

## Abstract

While deep reinforcement learning (RL) algorithms have been successfully applied to many tasks, their inability to extrapolate and strong reliance on episodic resets inhibits their applicability to many real-world settings. For instance, in stochastic queueing problems, the state space can be unbounded and the agent may have to learn online without the system ever being reset to states the agent has seen before. In such settings, we show that deep RL agents can diverge into unseen states from which they can never recover due to the lack of resets, especially in highly stochastic environments. Towards overcoming this divergence, we introduce a Lyapunov-inspired reward shaping approach that encourages the agent to first learn to be stable (i.e. to achieve bounded cost) and then to learn to be optimal. We theoretically show that our reward shaping technique reduces the rate of divergence of the agent and empirically find that it prevents it. We further combine our reward shaping approach with a weight annealing scheme that gradually introduces optimality and log-transform of state inputs, and find that these techniques enable deep RL algorithms to learn high performing policies when learning online in unbounded state space domains.

## 1 Introduction

Many deep reinforcement learning (RL) algorithms have been designed using environments [20, 9] that satisfy two criteria: (i) the state space is bounded, that is, the agent will only experience a bounded range of numeric inputs; (ii) the environment is episodic and resets are cheap; that is, the agent will periodically be reset to some distribution of initial states. However, many real-world applications violate these criteria and have the following characteristics:

- (i) The state space and range of inputs can be unbounded;
- (ii) Resets are difficult if not infeasible, requiring expensive manual or engineering efforts.

For example, in the load-balancing problem, the number of jobs waiting in a queue may grow arbitrarily large [45]; in traffic intersection management, the number of vehicles may increase without bound; in robotics, the robot may move far away from the initial condition.<sup>1</sup> In all these examples, resetting the system (e.g., removing all vehicles at a traffic intersection) is very costly or even inappropriate, particularly when a good simulator is absent and learning must be done in the real system [46].

Therefore, we need RL algorithms to be robust to potentially unbounded inputs and be able to learn quickly without the benefit of being periodically reset. In this paper, we demonstrate that current deep

---

<sup>1</sup>Even though the physics of the system may sometimes impose a finite limit on the state space (e.g., due to the physical space in a road intersection), the limit is often so large that the problem is virtually unbounded and foils existing methods (as we demonstrate momentarily).

RL algorithms are ill-equipped to learn in a single, long episode (i.e., continuing task RL [47, 46]) when the state-space is unbounded. We then identify several key techniques which when combined, make deep RL algorithms able to solve this challenging class of problems.

**Challenges.** Why do state space boundedness and resets make learning easier? The bounded state space alleviates the burden of extrapolation (i.e., generalization to states that are out of the range of previously seen states), which is especially challenging in deep RL where neural networks are notorious for poor extrapolation [54, 25, 4]. Meanwhile, episode resets allow an RL agent to go back to a set of previously observed states and apply what was learned in earlier episodes.

When these assumptions are relaxed, we find that many existing methods fail spectacularly and cannot even keep the system *stable*. That is, the agent *diverges*: it first encounters a state in which it has poor estimates of the optimal actions, it then makes a mistake, which makes it even more likely to encounter a new state in which it also has a poor estimate, and so on. The unboundedness of the state space means that there will always be a state that is unvisited by the agent; thus the agent may have to generalize in *unseen* states even before it has learned what to do in *seen* states. The lack of resets makes it difficult for the agent to refine its estimate of the optimal actions in previously encountered states. Therefore, the agent may never learn how to behave competently, let alone optimally, in any state. This divergence is drastically more pronounced in real-world settings where environment dynamics are highly stochastic.

**Contributions.** Our contributions are three-fold and are summarized as follows:

1. We empirically show that existing deep RL methods are unable to solve continuing tasks with unbounded state spaces. Particularly in highly stochastic environments, these methods typically lead to divergence. Common heuristics such as state space truncation do not eliminate the divergence.
2. We introduce Stability Then OPTimality (STOP), an approach that prevents divergence and explicitly encourages the agent to re-visit states and incur a bounded cost. The key idea of STOP is that it enables the agent to obtain useful signals for refining its estimation of the optimal actions—even when the *current* policy is unstable and diverging—thus serving as a first step towards optimality. Specifically, STOP consists of the following techniques: 1) a Lyapunov-inspired reward shaping approach that encourages the agent to be *stable* (i.e., achieve bounded cost [45]), 2) a weight annealing scheme that prioritizes first learning stability and then gradually shifting towards optimality, and 3) state transformations that reduce the rate at which the unbounded quantities of the state can diverge.
3. We conduct a thorough empirical study and analyze different components of STOP on challenging real-world-inspired domains.

See Section 6 for additional discussion of prior work on continuing RL and unbounded state spaces.

## 2 Preliminaries

Consider an infinite-horizon Markov decision process (MDP) [39],  $\mathcal{M} := \langle \mathcal{S}, \mathcal{A}, \mathcal{C}, \mathcal{P}, d_0 \rangle$ , where  $\mathcal{S} \subseteq \mathbb{R}^d$  is the state space,  $\mathcal{A}$  the action space,  $c : \mathcal{S} \times \mathcal{A} \times \mathcal{S} \rightarrow \mathbb{R}_{\geq 0}$  the cost function,  $\mathcal{P} : \mathcal{S} \times \mathcal{A} \rightarrow \Delta(\mathcal{S})$  the transition dynamics, and  $d_0 \in \Delta(\mathcal{S})$  the initial state distribution. Here we follow the control-theoretic convention and consider costs, which are the negation of rewards. Without loss of generality, we often restrict to cost-functions that are only dependent on the current state,  $s_t$ .

In the continuing task formulation, an agent, acting according to policy  $\pi : \mathcal{S} \rightarrow \Delta(\mathcal{A})$ , generates a *single* infinitely long trajectory:  $s_0, a_0, s_1, c_0, a_1, s_2, \dots$ , where  $s_0 \sim d_0$ ,  $a_t \sim \pi(\cdot | s_t)$ ,  $c_t = c(s_t, a_t, s_{t+1})$ , and  $s_{t+1} \sim \mathcal{P}(\cdot | s_t, a_t)$ . Unlike typical settings in RL, there are no resets in this formulation. Accordingly, we consider the long-run average-cost objective [37, 36]:

$$J^O(\pi) := \lim_{T \rightarrow \infty} \frac{1}{T} \sum_{t=1}^T \mathbb{E}_\pi [c(s_t, a_t, s_{t+1})]. \quad (1)$$

The goal is to find an optimal policy that minimizes  $J^O(\pi)$ . Note that a necessary condition for optimality is stability, i.e.,  $J^O(\pi) < \infty$ . Also we define the *differential* action-value function:  $Q^\pi(s, a) := \lim_{T \rightarrow \infty} \mathbb{E}_\pi [\sum_{t=0}^T (c(s_t) - J^O(\pi)) | s_0 = s, a_0 = a]$ .

In this work, we make the following technical assumptions:

**Assumption 1** (Communicating Assumption). *There exists a policy that can transition from any state to any other state in a finite number of steps with non-zero probability.*

**Assumption 2** (Bounded increment). *There exists a constant  $B < \infty$  such that  $\mathbb{E}_{s' \sim \mathcal{P}(\cdot|s,a)} |c(s') - c(s)| \leq B, \forall (s, a) \in \mathcal{S} \times \mathcal{A}$ .*

**Assumption 3** (Norm equivalence). *The cost function satisfies  $\underline{h}(\|s\|) \leq c(s, a, s') \leq \bar{h}(\|s\|), \forall (s, a, s')$  for some linear functions  $\underline{h}$  and  $\bar{h}$ , where  $\|\cdot\|$  is an arbitrary norm of the state.*

Assumption 1 is standard for average-cost problems [39, 7]; it ensures that there exists a policy  $\pi$  such that  $J^O(\pi)$  is independent of the initial state. Assumption 2 is a mild regularity condition satisfied by most practical problems. Assumption 3 implies that stability (resp., divergence) in the state is equivalent to stability (resp., divergence) in the cost; consequently, we do not distinguish these two notions, which simplifies the presentation in the sequel.

### 3 Deep RL in Continuing Tasks with Unbounded State-Spaces

In this section, we describe the core challenges that arise for deep RL agents when learning to solve a continuing task with an unbounded state space.

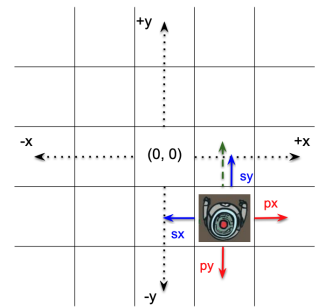
**Unbounded State Spaces** A bounded state space, even when continuous and infinite, mitigates the extrapolation burden on neural networks [54, 25, 4]. The agent can leverage the strong interpolation capability of neural networks to interpolate between the boundaries of the state space. For example, the angle of a robotic arm is between  $[0, 2\pi]$  and can take on infinitely many values, but a neural network will only be inputted values from this fixed range. However, when the state space is unbounded, the neural network is forced to make predictions in unseen regions of the state space, and the poor extrapolation leads to poor performance.

**Continuing Tasks** The ability to reset is heavily relied upon by many RL algorithms to learn performant policies. When an agent can be reset to a set of initial states, it is able to revisit states and improve its estimation of the optimal actions in those states. In the continuing setting [46, 10, 36], the agent is never reset. The agent must refine its estimation of the optimal actions on-the-fly, and it is evaluated based on its real-time performance.

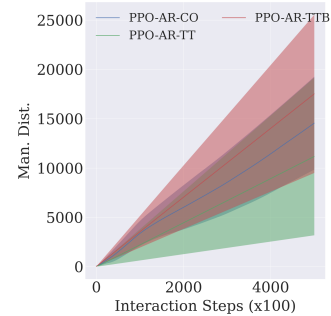
As we argue in Section 1, when the above assumptions are relaxed, the agent may diverge, as it is forced to extrapolate and is never given the opportunity to apply what it has learned. The problem is further exacerbated when the environment is highly stochastic and the cost function is poorly shaped.

To empirically illustrate the difficulty of learning in this setting, we consider an Infinite Gridworld domain where the axes are unbounded in the positive and negative directions; see Figure 1(a). In this domain, an agent is randomly spawned within some region of the grid and must try to move towards the origin by selecting between two actions: moving vertically or horizontally towards the goal. The state of the agent is the unbounded 2D coordinate location of the agent. With probabilities  $p_x = 0.2, p_y = 0.15$  the agent is pushed away from the origin along the respective axis. After an agent selects an axis to move along, its movement along that axis will be successful with probability  $s_x = 0.3, s_y = 0.8$  for the respective axis; if it fails to move, it will stay in the same location unless pushed away. The cost function is the Manhattan distance between the agent and the origin.

Despite the domain’s simplicity, we find existing RL algorithms are unable to solve this task. In Figure 1(b), we plot Manhattan distance vs. interaction time of three well-tuned average-reward



(a)



(b)

Figure 1: (a) Infinite gridworld environment. (b) Performance measured in Manhattan distance from origin vs. interaction steps. Results are over 5 trials and show the 95% confidence interval. Refer to main text for descriptions of the algorithms.

Proximal Policy Optimization (PPO) agents [58] equipped with best-practice optimizations [18]: 1) PPO-AR-CO: a PPO agent that starts from a random policy and learns as it interacts with the environment (an example of [46, 47]’s continuing setting), 2) PPO-AR-TT: a PPO agent that is first trained in a setting where the agent gets reset after 30K time-steps, and then it is deployed on the actual continuing task, and 3) PPO-AR-TTB: a PPO agent that is trained and tested the same way as PPO-AR-TT, but during the *training* phase, the state space is artificially truncated to be between  $[-1000, 1000]$ . As we can see, for all methods, the distance from the origin grows arbitrarily large.

We highlight the failures of PPO-AR-TT and PPO-AR-TTB: even if one can reset or truncate the state space *during training* (which are common practices when, e.g., a simulator is available), the agent still fails when deployed for the actual task. In Section 5 we provide additional examples, including a traffic control domain where the state space is finite but large and the above methods still perform poorly. These results show that unbounded spaces and continuing tasks are not merely a theoretical inconvenience, but they pose fundamental challenges to deep RL.

## 4 STOP: Stability Then Optimality

We now turn to the question of how to make deep RL succeed in the unbounded state space and continuing setting. We introduce our method, Stability Then OPTimality (STOP), which is based on the key insight of first encouraging stability (i.e., keeping the state and cost bounded) and then optimality. STOP consists of three ingredients: 1) reward shaping to encourage stability, 2) reverse-annealing the optimality cost, and 3) state transformations. All three ingredients are algorithm-agnostic and can be adopted within any RL algorithm, including but not limited to PPO.

### 4.1 Stability through Reward Shaping

In principle, minimizing the average-cost optimality criterion  $J^O$ , defined in (1), should result in optimal performance. However,  $J^O$  is difficult to minimize directly; even keeping  $J^O$  bounded is challenging, as we have seen in Figure 1(b). In this infinite gridworld case, once the cost (Manhattan distance) is high, the agent is unable to make progress as it cannot distinguish between good and bad actions, as their difference is vanishingly small compared to the (currently) large cost. Furthermore, even if the cost function is clipped [18], the agent will be unable to distinguish between good and bad actions once the cost function crosses the clip limit as all cost incurred are the same. This inability is exacerbated in continuing environments where the agent must learn to make progress quickly.

To facilitate learning, we propose to use reward shaping, with the following intuition: the shaping reward should encourage the agent to be *stable* i.e., to not diverge and to incur bounded cost. A stable agent will be able to repeatedly revisit states and improve its estimates of the optimal actions. Once the agent is stable, it can start to optimize the original optimality objective  $J^O$ . To encourage stability, we design the following cost function as the difference between consecutive costs, i.e.,  $g(s_{t-1}, s_t) := c(s_t) - c(s_{t-1})$ . That is, the agent is rewarded for moving to a state in which it will incur a cost less than what it incurred in the previous time-step. While straightforward, this approach has far-reaching consequences: 1)  $g(s_{t-1}, s_t)$  is always bounded, 2) it induces a well-defined policy gradient even when the current policy is unstable, and 3) it provides immediate feedback on progress and encourages stability. We provide theoretical justifications for these properties in Section 4.1.1.

We remark that the above approach can be generalized to the form  $g(s_{t-1}, s_t) := \ell(s_t) - \ell(s_{t-1})$ , where  $\ell : \mathcal{S} \rightarrow \mathbb{R}_{\geq 0}$  is any *Lyapunov function* [55, 45] satisfying  $\liminf_{\|s\| \rightarrow \infty} \ell(s) = \infty$ . Minimizing  $g$  thus amounts to minimizing the *drift* of the Lyapunov function. Lyapunov functions are a standard tool in the *analysis* of stochastic systems, and it is well-known that a negative Lyapunov drift is a sufficient condition for stochastic stability [35]. Here we use it *algorithmically*.

#### 4.1.1 Theoretical Results

To investigate the theoretical properties of the stability cost function  $g$ , we consider the corresponding average-cost objective:

$$J^S(\pi) := \lim_{T \rightarrow \infty} \frac{1}{T} \sum_{t=1}^T \mathbb{E}_\pi g(s_{t-1}, s_t) = \lim_{T \rightarrow \infty} \frac{1}{T} \sum_{t=1}^T \mathbb{E}_\pi [c(s_t) - c(s_{t-1})]. \quad (2)$$

Later we will use  $J^S$  as a *regularizer* and combine it with the original optimality criterion  $J^O$

Our first lemma shows that  $J^S(\pi)$  is always bounded and well-defined, regardless of whether  $\pi$  is stable. This follows from the fact that  $\mathbb{E}_\pi c(s_t)$  cannot grow faster than linearly under Assumption 2.

**Lemma 1.** (*Boundedness of  $g$  and  $J^S$* ) Under Assumptions 1 and 2, we have  $\mathbb{E}_\pi [g(s_{t-1}, s_t)] \leq B, \forall t$  and  $J^S(\pi) \leq B$  for all policies  $\pi$ .

We now define a new MDP, denoted by  $\mathcal{M}^S$ , with state  $x_t = (s_{t-1}, s_t)$  (i.e., a concatenation of two successive states) and instantaneous cost function  $g(x_t) = c(s_t) - c(s_{t-1})$ , in which case  $J^S(\pi)$  is the corresponding average-cost objective of  $\mathcal{M}^S$ . Since  $g$  and  $J^S$  are always bounded (Lemma 1), the action-value function, denoted by  $Q_{\mathcal{M}^S}^\pi$ , is well defined for all policies  $\pi$  under  $\mathcal{M}^S$ . Using this connection, the proposition below characterizes the policy gradient of  $J^S$ .

**Proposition 1.** (*Policy gradient of  $J^S$* ) Consider a policy class  $\{\pi_\theta\}$  smoothly parameterized by  $\theta$ . Under Assumptions 1 and 2, for any  $\theta$ , the policy gradient is well-defined and admits the expression

$$\frac{d}{d\theta} J^S(\pi_\theta) = \mathbb{E}_\pi [Q_{\mathcal{M}^S}^{\pi_\theta}((s_{t-1}, s_t), a_t) \nabla_\theta \log \pi_\theta(a_t | s_t)].$$

For tabular or softmax parametrization, policy gradient methods applied to  $J^S$  converge to its global minimizers (despite nonconvexity) [2]; see [8] for other sufficient conditions of global convergence.

We say that the system is *rate-stable in mean* under the policy  $\pi$  if  $\lim_{T \rightarrow \infty} \frac{1}{T} \mathbb{E}_\pi \|s_T\| = 0$ , that is,  $\mathbb{E}_\pi \|s_T\| = o(T)$ . Rate-stability (a.k.a. pathwise-stability) is a standard criterion in the queueing and stochastic network literature [13, 17]. Our last proposition shows that minimizing  $J^S$  gives rate-stable policies. There are other formal notions of stability [35, 45]; we leave it to future work to study the relationship between these alternative notions and our reward shaping approach.

**Proposition 2.** ( *$J^S$  and rate stability*) Under Assumptions 1–3,  $\min_\pi J^S(\pi) = 0$ . Moreover, the system is rate-stable in mean under  $\bar{\pi}$  if and only if  $\bar{\pi} \in \arg \min_\pi J^S(\pi)$ .

Due to space constraints, we defer the proofs to Appendix A.

## 4.2 Applying Stability + Optimality with Reverse Annealing

Minimizing the shaped cost function  $g$  encourages the agent to learn a stable policy. While this ensures a bounded average cost w.r.t.  $c$ , the cost itself may be high. To further reduce the cost, the learning agent must also pursue optimality i.e. the original objective  $J^O$ . So that the agent first incurs bounded costs and then pursues optimal costs, we set the agent’s objective at time-step  $\tau$  to be:

$$\min_\pi \lim_{T \rightarrow \infty} \frac{1}{T} \sum_{t=1}^T \mathbb{E}_\pi \left[ \underbrace{c(s_t) - c(s_{t-1})}_{\substack{\text{stability cost} \\ g(s_{t-1}, s_t)}} + \lambda(\tau) \underbrace{\left( \frac{-1}{c(s_t) + 1} \right)}_{\substack{\text{optimality cost}}} \right]. \quad (3)$$

Note that the first part of the above objective is simply the stability objective  $J^S$ . One may view  $J^S$  as a regularizer, which encourages stability throughout the interaction process.

The coefficient  $\lambda(\tau)$  in (3) is reverse annealed as a function of the time  $\tau$  to increase emphasis on the optimality term over time. Specifically, we use the annealing schedule:  $\lambda(\tau) = \tanh(\beta \max(\tau - \tau_{\text{warmup}}, 0.01))$ , where  $\beta$  determines the speed at which  $\lambda$  reaches 1 (its maximum value) and  $\tau_{\text{warmup}}$  determines at what time-step in the interaction process that  $\lambda$  starts taking effect [32].

Note that at time-step  $t$  the agent minimizes  $\frac{-1}{c(s_t)+1}$  instead of  $c(s_t)$ , since the unbounded nature of the latter may: 1) dilute the stability cost due to different cost scales and 2) erase information the agent has learned thus far due to large gradient updates. Here we take the reciprocal of  $c(s_t)$  to keep it on the same scale as the stability cost.

By solving the optimization in Eq. (3) the agent first learns to be stable and then learn to be optimal. Since an optimal policy  $\pi^*$  is by definition stable and satisfies  $J^S(\pi^*) = 0$ , the minimizer of the objective (3) will be the same as the optimal policy w.r.t. the original optimality criterion  $J^O$ .

## 4.3 State Transformations

The above stability reward and weight annealing scheme are sufficient in many cases to learn a good stable policy. To further optimize performance, especially in highly stochastic environments, we find

that another important consideration for deep RL is to transform the state input into the policy, so that the rate of divergence of the unbounded quantities decreases.

We consider transformation functions that: 1) reduce divergence of the unbounded quantities and 2) preserve the ordering between unbounded quantities. In particular, we experimented with symmetric square root:  $\text{symsqrt}(x) := \text{sign}(x)(\sqrt{|x| + 1} - 1)$  [28], symmetric natural log:  $\text{symloge}(x) := \text{sign}(x)\ln(|x| + 1)$  [24], and symmetric base 10 log:  $\text{symlog10}(x) := \text{sign}(x)\log_{10}(|x| + 1)$  (see Figure 5 in Appendix B). Intuitively, these transformations mitigate some of the extrapolation burden as states appear closer to one another and the agent observes less extreme values. Empirically, we find that these transformations significantly improves an agent’s ability to learn a stable policy with low costs. Note that we apply these transformations coordinate-wise to the states only before inputting them into the policy and value networks; the cost function is computed based on the original state.

## 5 Empirical Study

In this section, we present an empirical study of STOP on real-world-inspired continuing tasks with unbounded state spaces and high stochasticity. We design our empirical study to answer the questions:

1. Does STOP improve the robustness of RL algorithms in this difficult setting?
2. How long should STOP optimize for stability before pursuing optimality?
3. How do different state transformations impact the performance of STOP?

### 5.1 Setup

We first describe the environments, the algorithms we evaluate, and how we evaluate performance. We refer the reader to Appendix B for more details.

**Environments** We conduct our experiments on the following environments:

**2D goal-reaching infinite gridworld:** This domain was introduced in Section 3. We use the change-in-Manhattan distance as the stability cost function.

**Single-server allocation queuing:** At each time-step the server must select from a set of queues to serve. High stochasticity is due to job arrivals, failure in successfully serving a queue, and faulty connections. The state is the queue lengths of each queue and 0/1 flags indicating connectivity to each queue. The action is the index of a given queue. The dimensions of the state and action space are  $2N$  and  $N$  respectively, where  $N$  is the number of queues. The optimality criterion is to minimize the average queue lengths. We use the change-in-queue-length as the stability cost function. Note that the optimal policy in the faulty connection setting is unknown and is an open problem, so the optimal policy cannot be determined even when the transition dynamics are known [21]. As we will see in the following experiments, a smaller queue setting with faulty connections can be significantly harder than a larger queue setting with no faulty connections.

**Traffic control:** At each time-step a traffic controller must select a set of non-conflicting lanes to allow traffic. At each time-step, new cars arrive stochastically. We use the SUMO simulator implementation [5, 3], and we experiment with varying levels of traffic congestion on a given intersection design. The state is the number of cars in each lane along with indicator flags for the different light colors (green, yellow, red) and action is the index of which set of lanes are permitted to move. The dimensions of the state and action space are 21 and 4 dimensions respectively. The optimality criterion is to minimize the total waiting time across all cars. We use the change-in-waiting-time as the stability cost function. In this domain, SUMO models a real-life traffic situation by imposing a cap on the number of cars per lane. However, as we will show, deep RL algorithms still fail despite this cap.

**Algorithms** While in principle, our approach is compatible with any RL algorithm, we focus on the average-reward versions of PPO and TRPO (Trust-Region Policy Optimization) [59, 43, 42] due to their widespread use and robust performance.

**Online Evaluation and Training Procedure** Unlike other work that evaluates RL agents by first resetting the agent and then observing its performance, we keep track of the *online* performance of the agent as it interacts with the environment until the end of the experiment. The agent starts from a

random start state and with a randomly-initialized policy and is never reset. The performance of the agent is the *real-time* performance of the agent according to the *true* optimality criterion. The agent updates its policy every 512 time-steps using the data it has collected since the last update.

## 5.2 Main Results

We now present our main results after integrating STOP with PPO and TRPO. We sweep over the hyperparameters  $\tau_{\text{warmup}}$  and  $\beta$  for agents that optimize stability and optimality (Eq. (3)). All algorithm variations of STOP (stability-only and stability+optimality) apply the symloge transform and use the same PPO/TRPO hyperparameters [40].

In all experiments, the naïve PPO and TRPO agents, which optimized the optimality criterion directly, performed significantly worse compared to variations of our approach. In environments with high stochasticity, such as the 2-queue network, optimizing only the stability reward is insufficient for TRPO and the agent starts to perform poorly. However, in general including the stability reward substantially reduces the Manhattan distance, average queue length, and total waiting time, and including optimality tends to further improve performance.

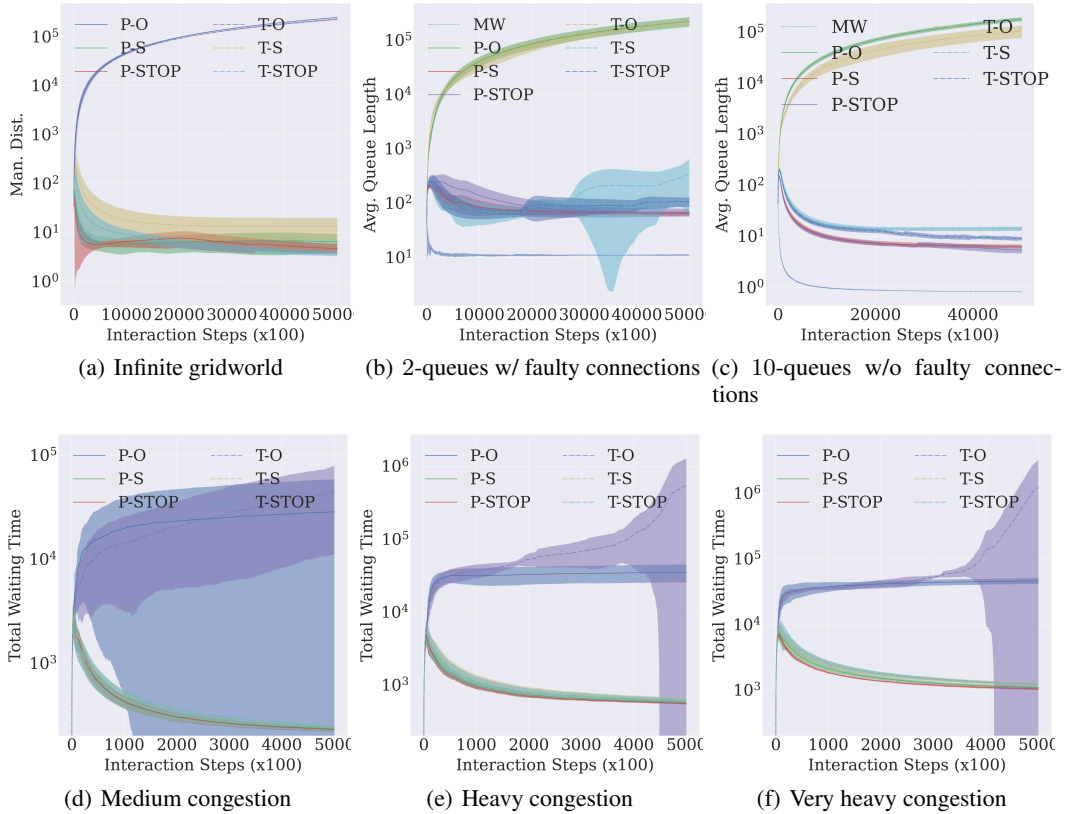


Figure 2: True optimality criterion vs. interaction time-steps on infinite gridworld, two queue networks variants, and traffic control environment for average-reward TRPO (T-) and PPO (P-). Lower is better. (-O), (-S), and (-SO) indicate the algorithm optimizes optimality only, stability only, and stability+optimality respectively. For the queueing environment, we also report the performance a heuristic-based algorithm called MaxWeight (MW). Performance metrics are computed over 5 trials with 95% confidence intervals. The vertical axis is log-scaled.

## 5.3 Ablation Studies

In our ablation studies, we evaluate the impact of different components of STOP: the weight schedule parameters  $\tau_{\text{warmup}}$  and the state transformation functions. We show ablations on the 10-queue and 2-queue network systems.

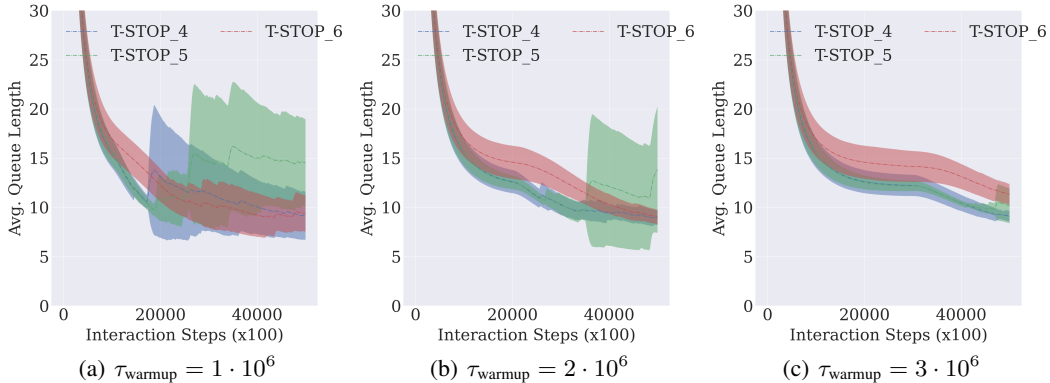


Figure 3: Average queue length vs. interaction time-steps on the 10-queue network for different values of  $\tau_{\text{warmup}}$ . The legend is read as T-STOP- $\langle\beta\rangle$  as the exponent. For example, for T-STOP-6,  $\beta = 10^{-6}$ . Performance metrics are computed over 5 trials with 95% confidence intervals. Lower is better.

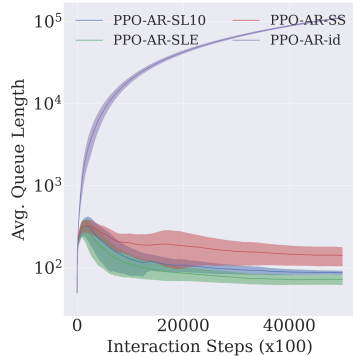
### 5.3.1 Varying $\tau_{\text{warmup}}$

We found STOP PPO to be robust to this hyperparameter so we show results only for STOP TRPO. From Figure 3, we generally find that regardless of the speed ( $\beta$ ) at which optimality is introduced, introducing optimality later on in the interaction process (larger  $\tau_{\text{warmup}}$ ) tends to achieve lower cost at lower variance. This result suggests it is critical for the agent to first achieve stability and then pursue optimality. Otherwise, the optimality criterion can distract the agent causing it to make mistakes.

Due to space constraints, we defer the results on variation of  $\beta$  to the Appendix B. From those experiments, we reach the same conclusion: it is important to let the agent first be stable and then be optimal by gradually introducing optimality for better performance at lower variance.

### 5.3.2 Varying State Transformations

In this experiment, we see the performance of the STOP PPO agent with different state transformations applied to the unbounded state space. From Figure 4, applying state transformations that satisfy the criteria in Section 4.3 results in significantly better performance compared to no application of such a transformation. However, we also observe that if the transformation severely squishes its inputs such as  $\text{symlog}_{10}$ , it may hurt the agent’s performance since the outputs of the transformation look the same, thus making it difficult for the agent to distinguish between states.



## 6 Related Work

In this section we review prior work related to continuing RL and stability in unbounded state spaces.

**Continuing Reinforcement Learning** Our work focuses on learning under the continuing RL task definition in which interaction never terminates and performance is measured online [47]. This problem setting has also recently been described with the autonomous RL [46] formalism. Another related formalism is single-life RL [10], which assumes the learning agent has a prior dataset of offline experience to draw from during learning. In many practical RL set-ups, it may be infeasible to reset the learning agent to a new initial state after an episode ends. To address this challenge, recent work has considered *reset-free* RL in which the learning agent also learns to reset itself before its next attempt at a task [19, 60, 23, 26]. However, these works still require a manual reset [19] or use policies learned on one

Figure 4: Performance of STOP applied to PPO as a function of state transformations: identity (-id), symmetric squareroot (-SS), symmetric natural log (-SLE), and symmetric log (-SL10) on the 2-queue server allocation problem w/ faulty connections. Lower is better. The vertical axis is log-scaled.



task as an approximate reset policy in another task through multi-tasking learning [23]. Our work, on the other hand, performs no resets and is concerned with performance on a single infinitely-long task.

In continuing RL, the natural performance measure of an agent is average-reward [47, 37]. Despite a long history [33, 44], average-reward reinforcement learning has received comparably less attention compared to the discounted, episodic return objective. Nonetheless, several recent works have made progress in developing deep RL algorithms for average-reward RL [50, 52, 59, 57] In contrast to these works, our work tackles the challenge of unbounded state spaces.

To avoid a possible point of confusion, we emphasize that our work focuses on *continuing* RL and not *continual* RL. The latter tends to address non-stationarity of the task being faced by the learning agent and much work in continual RL still uses an episodic task formulation. Our setting, on the other hand, assumes that the agent is solving *one* task with stationary dynamics in a *single* episode.

**Stability and Unbounded State Spaces in Reinforcement Learning** The concept of stability in reinforcement learning has largely been overlooked. Stability is related to the notion of *safety* in RL [22], but with crucial differences. Safety is typically defined as hard constraints on individual states and/or actions [27, 14, 15, 29], or soft constraints on the expected costs over the trajectory [1, 11, 56]. In contrast, stability concerns the long-run asymptotic behavior of the system, which cannot be immediately written as constraints over the state/action or budget on some cost.

It is worth mentioning that some work considers control-theoretic notions of stability [49, 6], which is related to our setting. However, these results mostly focus on systems with deterministic and partially unknown dynamics. For example, [53] also proposes a cost-shaping approach, which bears similarities to ours. However, their problem setting is quite different: they focus on deterministic dynamics and a different notion of stability (asymptotic stability); they consider discounted costs, and do not study the continuing setting with unbounded state spaces.

The work [45] introduced stability as a first step towards making RL training feasible in the unbounded state space setting. However, 1) their work was largely theoretical and made the tabular setting assumption, 2) they relied on access to the model of the environment to conduct simulations, and 3) they ignored optimality and focused exclusively on stability. Our work, on the other hand, makes stability practical for deep RL, makes no assumptions on having access to the environment model, and combines stability with optimality. In the few works that do consider stability [12, 31], they assume that a stable policy is given and use it as a starting point for learning an optimal policy. Instead we make no such assumption and try to learn a stable policy directly from a random policy.

The unbounded state space and continuing setting is also scarce in the RL literature. Existing works acknowledge the difficulties in handling the unbounded states, but they either artificially bound the state space [31], or consider unbounded state spaces but assume the episodic training setting [12].

## 7 Conclusion

In our work, we considered a unique and difficult setting: a continuing task (no resets) with unbounded state spaces and high stochasticity. We demonstrated evidence showing that current RL algorithms are unable to solve these tasks. We then introduced STOP, an approach based on: 1) stability, 2) reverse annealing of the optimality criterion, and 3) state transformations to make learning possible. Our work is novel in that it tackles this setting directly on challenging real-world-inspired domains and proposes STOP as a technique to build robust and highly performant RL policies in a difficult setting that has largely been overlooked in the literature.

### 7.1 Limitations and Future Work

We highlight some limitations and directions for future work. Despite mitigating the burden of extrapolation of neural networks through reward shaping and state transformations, they are still fundamentally poor at extrapolation. An open question still remains as to how to improve extrapolation of neural networks. Another exciting direction is to study the challenges that arise from non-stationary dynamics. With non-stationary dynamics, important challenges such as catastrophic forgetting [34] and primacy bias in deep RL [38] arise. A potential direction is to combine STOP with other forms of gradient descent [16] that try to overcome these challenges. In our work, we addressed fundamental research questions in RL, and thus we do not see any immediate negative societal impacts.

## References

- [1] Joshua Achiam, David Held, Aviv Tamar, and Pieter Abbeel. Constrained policy optimization. In *Proceedings of the 34th International Conference on Machine Learning-Volume 70*, pages 22–31. JMLR. org, 2017.
- [2] Alekh Agarwal, Nan Jiang, Sham M Kakade, and Wen Sun. *Reinforcement Learning: Theory and Algorithms*. 2021.
- [3] Lucas N. Alegre. SUMO-RL. <https://github.com/LucasAlegre/sumo-rl>, 2019.
- [4] E. Barnard and L.F.A. Wessels. Extrapolation and interpolation in neural network classifiers. *IEEE Control Systems Magazine*, 12(5):50–53, 1992.
- [5] Michael Behrisch, Laura Bieker-Walz, Jakob Erdmann, and Daniel Krajzewicz. Sumo – simulation of urban mobility: An overview. volume 2011, 10 2011.
- [6] Felix Berkenkamp, Matteo Turchetta, Angela Schoellig, and Andreas Krause. Safe model-based reinforcement learning with stability guarantees. In *Advances in neural information processing systems*, pages 908–918, 2017.
- [7] Dimitri P Bertsekas. Dynamic programming and optimal control, 4th edition, volume II. *Athena Scientific*, 2015.
- [8] Jalaj Bhandari and Daniel Russo. Global optimality guarantees for policy gradient methods. *arXiv preprint arXiv:1906.01786*, 2019.
- [9] Greg Brockman, Vicki Cheung, Ludwig Pettersson, Jonas Schneider, John Schulman, Jie Tang, and Wojciech Zaremba. Openai gym, 2016.
- [10] Annie S. Chen, Archit Sharma, Sergey Levine, and Chelsea Finn. You Only Live Once: Single-Life Reinforcement Learning, October 2022. arXiv:2210.08863 [cs].
- [11] Yinlam Chow, Ofir Nachum, Edgar Duenez-Guzman, and Mohammad Ghavamzadeh. A lyapunov-based approach to safe reinforcement learning. In *Advances in Neural Information Processing Systems*, pages 8092–8101, 2018.
- [12] J. G. Dai and Mark Gluzman. Queueing network controls via deep reinforcement learning. *Stochastic Systems*, 12(1):30–67, 2022.
- [13] JG Dai and Otis B Jennings. Stabilizing queueing networks with setups. *Mathematics of Operations Research*, 29(4):891–922, 2004.
- [14] Gal Dalal, Krishnamurthy Dvijotham, Matej Vecerik, Todd Hester, Cosmin Paduraru, and Yuval Tassa. Safe exploration in continuous action spaces. *arXiv preprint arXiv:1801.08757*, 2018.
- [15] Sarah Dean, Stephen Tu, Nikolai Matni, and Benjamin Recht. Safely learning to control the constrained linear quadratic regulator. In *2019 American Control Conference (ACC)*, pages 5582–5588. IEEE, 2019.
- [16] Shibhansh Dohare, Richard S. Sutton, and A. Rupam Mahmood. Continual backprop: Stochastic gradient descent with persistent randomness, 2022.
- [17] Muhammad El-Taha and Shaler Stidham Jr. *Sample-Path Analysis of Queueing Systems*, volume 11. Springer Science & Business Media, 2012.
- [18] Logan Engstrom, Andrew Ilyas, Shibani Santurkar, Dimitris Tsipras, Firdaus Janoos, Larry Rudolph, and Aleksander Madry. Implementation matters in deep rl: A case study on ppo and trpo. In *International Conference on Learning Representations*, 2020.
- [19] Benjamin Eysenbach, Shixiang Gu, Julian Ibarz, and Sergey Levine. Leave no Trace: Learning to Reset for Safe and Autonomous Reinforcement Learning. February 2018.
- [20] Justin Fu, Aviral Kumar, Ofir Nachum, George Tucker, and Sergey Levine. D4rl: Datasets for deep data-driven reinforcement learning, 2020.

- [21] Anand Ganti, Eytan Modiano, and John N. Tsitsiklis. Optimal transmission scheduling in symmetric communication models with intermittent connectivity. *IEEE Transactions on Information Theory*, 53(3):998–1008, March 2007.
- [22] Javier Garcia and Fernando Fernández. A comprehensive survey on safe reinforcement learning. *Journal of Machine Learning Research*, 16(1):1437–1480, 2015.
- [23] Abhishek Gupta, Justin Yu, Tony Z. Zhao, Vikash Kumar, Aaron Rovinsky, Kelvin Xu, Thomas Devlin, and Sergey Levine. Reset-Free Reinforcement Learning via Multi-Task Learning: Learning Dexterous Manipulation Behaviors without Human Intervention, April 2021. arXiv:2104.11203 [cs].
- [24] Danijar Hafner, Jurgis Pasukonis, Jimmy Ba, and Timothy Lillicrap. Mastering diverse domains through world models, 2023.
- [25] P.J. Haley and D. Soloway. Extrapolation limitations of multilayer feedforward neural networks. In *[Proceedings 1992] IJCNN International Joint Conference on Neural Networks*, volume 4, pages 25–30 vol.4, 1992.
- [26] Weiqiao Han, Sergey Levine, and Pieter Abbeel. Learning compound multi-step controllers under unknown dynamics. In *2015 IEEE/RSJ International Conference on Intelligent Robots and Systems (IROS)*, pages 6435–6442, September 2015.
- [27] Alexander Hans, Daniel Schneegaß, Anton Maximilian Schäfer, and Steffen Udluft. Safe exploration for reinforcement learning. In *ESANN*, pages 143–148, 2008.
- [28] Steven Kapturowski, Georg Ostrovski, Will Dabney, John Quan, and Remi Munos. Recurrent experience replay in distributed reinforcement learning. In *International Conference on Learning Representations*, 2019.
- [29] Torsten Koller, Felix Berkenkamp, Matteo Turchetta, and Andreas Krause. Learning-based model predictive control for safe exploration. In *2018 IEEE Conference on Decision and Control (CDC)*, pages 6059–6066. IEEE, 2018.
- [30] Bai Liu, Qiaomin Xie, and Eytan Modiano. Reinforcement learning for optimal control of queueing systems. In *2019 57th Annual Allerton Conference on Communication, Control, and Computing (Allerton)*, pages 663–670, 2019.
- [31] Bai Liu, Qiaomin Xie, and Eytan Modiano. RL-qn: A reinforcement learning framework for optimal control of queueing systems. *ACM Trans. Model. Perform. Eval. Comput. Syst.*, 7(1), aug 2022.
- [32] James MacGlashan, Evan Archer, Alisa Devlic, Takuma Seno, Craig Sherstan, Peter R. Wurman, and Peter Stone. Value function decomposition for iterative design of reinforcement learning agents. In Alice H. Oh, Alekh Agarwal, Danielle Belgrave, and Kyunghyun Cho, editors, *Advances in Neural Information Processing Systems*, 2022.
- [33] Sridhar Mahadevan. Average reward reinforcement learning: Foundations, algorithms, and empirical results. *Machine Learning*, 22(1):159–195, March 1996.
- [34] Michael McCloskey and Neal J. Cohen. Catastrophic interference in connectionist networks: The sequential learning problem. *Psychology of Learning and Motivation*, 24:109–165, 1989.
- [35] Sean P Meyn and Richard L Tweedie. *Markov chains and stochastic stability*. Springer Science & Business Media, 2012.
- [36] Abhishek Naik, Zaheer Abbas, Adam White, and Richard S. Sutton. Towards reinforcement learning in the continuing setting. 2021.
- [37] Abhishek Naik, Roshan Shariff, Niko Yasui, and Richard S. Sutton. Discounted reinforcement learning is not an optimization problem. *CoRR*, abs/1910.02140, 2019.

- [38] Evgenii Nikishin, Max Schwarzer, Pierluca D’Oro, Pierre-Luc Bacon, and Aaron Courville. The primacy bias in deep reinforcement learning. In Kamalika Chaudhuri, Stefanie Jegelka, Le Song, Csaba Szepesvari, Gang Niu, and Sivan Sabato, editors, *Proceedings of the 39th International Conference on Machine Learning*, volume 162 of *Proceedings of Machine Learning Research*, pages 16828–16847. PMLR, 17–23 Jul 2022.
- [39] Martin L Puterman. *Markov decision processes: discrete stochastic dynamic programming*. John Wiley & Sons, 2014.
- [40] Antonin Raffin, Ashley Hill, Adam Gleave, Anssi Kanervisto, Maximilian Ernestus, and Noah Dormann. Stable-baselines3: Reliable reinforcement learning implementations. *Journal of Machine Learning Research*, 22(268):1–8, 2021.
- [41] Stuart Russell and Andrew L. Zimdars. Q-decomposition for reinforcement learning agents. In *Proceedings of the Twentieth International Conference on International Conference on Machine Learning*, ICML’03, page 656–663. AAAI Press, 2003.
- [42] John Schulman, Sergey Levine, Pieter Abbeel, Michael Jordan, and Philipp Moritz. Trust region policy optimization. In Francis Bach and David Blei, editors, *Proceedings of the 32nd International Conference on Machine Learning*, volume 37 of *Proceedings of Machine Learning Research*, pages 1889–1897, Lille, France, 07–09 Jul 2015. PMLR.
- [43] John Schulman, Filip Wolski, Prafulla Dhariwal, Alec Radford, and Oleg Klimov. Proximal policy optimization algorithms. *CoRR*, abs/1707.06347, 2017.
- [44] Anton Schwartz. A Reinforcement Learning Method for Maximizing Undiscounted Rewards. pages 298–305, December 1993.
- [45] Devavrat Shah, Qiaomin Xie, and Zhi Xu. Stable reinforcement learning with unbounded state space. In Alexandre M. Bayen, Ali Jadbabaie, George Pappas, Pablo A. Parrilo, Benjamin Recht, Claire Tomlin, and Melanie Zeilinger, editors, *Proceedings of the 2nd Conference on Learning for Dynamics and Control*, volume 120 of *Proceedings of Machine Learning Research*, pages 581–581. PMLR, 10–11 Jun 2020.
- [46] Archit Sharma, Kelvin Xu, Nikhil Sardana, Abhishek Gupta, Karol Hausman, Sergey Levine, and Chelsea Finn. Autonomous reinforcement learning: Formalism and benchmarking. *ArXiv*, abs/2112.09605, 2021.
- [47] Richard S. Sutton and Andrew G. Barto. *Reinforcement Learning: An Introduction*. A Bradford Book, Cambridge, MA, USA, 2018.
- [48] Richard S Sutton, David McAllester, Satinder Singh, and Yishay Mansour. Policy gradient methods for reinforcement learning with function approximation. *Advances in neural information processing systems*, 12, 1999.
- [49] Julia Vinogradskaa, Bastian Bischoff, Duy Nguyen-Tuong, Anne Romer, Henner Schmidt, and Jan Peters. Stability of controllers for gaussian process forward models. In *International Conference on Machine Learning*, pages 545–554, 2016.
- [50] Yi Wan, Abhishek Naik, and Richard S. Sutton. Learning and Planning in Average-Reward Markov Decision Processes. In *Proceedings of the 38th International Conference on Machine Learning*, pages 10653–10662. PMLR, July 2021. ISSN: 2640-3498.
- [51] Yi Wan, Abhishek Naik, and Richard S Sutton. Learning and planning in average-reward markov decision processes. In Marina Meila and Tong Zhang, editors, *Proceedings of the 38th International Conference on Machine Learning*, volume 139 of *Proceedings of Machine Learning Research*, pages 10653–10662. PMLR, 18–24 Jul 2021.
- [52] Chen-Yu Wei, Mehdi Jafarnia-Jahromi, Haipeng Luo, Hiteshi Sharma, and Rahul Jain. Model-free Reinforcement Learning in Infinite-horizon Average-reward Markov Decision Processes, February 2020. arXiv:1910.07072 [cs, stat].

- [53] Tyler Westenbroek, Fernando Castaneda, Ayush Agrawal, Shankar Sastry, and Koushil Sreenath. Lyapunov design for robust and efficient robotic reinforcement learning. In *6th Annual Conference on Robot Learning*, 2022.
- [54] Keyulu Xu, Mozhi Zhang, Jingling Li, Simon Shaolei Du, Ken-Ichi Kawarabayashi, and Stefanie Jegelka. How neural networks extrapolate: From feedforward to graph neural networks. In *International Conference on Learning Representations*, 2021.
- [55] Kuang Xu. *Drift Method: from Stochastic Networks to Machine Learning*.
- [56] Ming Yu, Zhuoran Yang, Mladen Kolar, and Zhaoran Wang. Convergent policy optimization for safe reinforcement learning. In *Advances in Neural Information Processing Systems*, pages 3121–3133, 2019.
- [57] Shangdong Zhang, Yi Wan, Richard S. Sutton, and Shimon Whiteson. Average-Reward Off-Policy Policy Evaluation with Function Approximation. In *Proceedings of the 38th International Conference on Machine Learning*, pages 12578–12588. PMLR, July 2021. ISSN: 2640-3498.
- [58] Yiming Zhang and Keith W. Ross. On-Policy Deep Reinforcement Learning for the Average-Reward Criterion, June 2021. arXiv:2106.07329 [cs, stat].
- [59] Yiming Zhang and Keith W Ross. On-policy deep reinforcement learning for the average-reward criterion. In Marina Meila and Tong Zhang, editors, *Proceedings of the 38th International Conference on Machine Learning*, volume 139 of *Proceedings of Machine Learning Research*, pages 12535–12545. PMLR, 18–24 Jul 2021.
- [60] Henry Zhu, Justin Yu, Abhishek Gupta, Dhruv Shah, Kristian Hartikainen, Avi Singh, Vikash Kumar, and Sergey Levine. The Ingredients of Real-World Robotic Reinforcement Learning, April 2020. arXiv:2004.12570 [cs, stat].

## A Theoretical Results

In this section we provide the proofs for our theoretical results, which are restated below for readers' convenience. The starting point of our proofs is to rewrite the stability objective  $J^S$  as follows:

$$\begin{aligned} J^S(\pi) &= \lim_{T \rightarrow \infty} \frac{1}{T} \sum_{t=1}^T (\mathbb{E}_\pi c(s_t) - \mathbb{E}_\pi c(s_{t-1})) \\ &= \lim_{T \rightarrow \infty} \frac{1}{T} (\mathbb{E}_\pi c(s_T) - \mathbb{E}_\pi c(s_0)) \\ &\stackrel{(i)}{=} \lim_{T \rightarrow \infty} \frac{1}{T} \mathbb{E}_\pi c(s_T), \end{aligned}$$

where the equality (i) holds since  $\mathbb{E}_\pi c(s_0)$  is independent of  $T$ .

**Lemma 1.** (Boundedness of  $g$  and  $J^S$ ) Under Assumptions 1 and 2, we have  $\mathbb{E}_\pi[g(s_{t-1}, s_t)] \leq B, \forall t$  and  $J^S(\pi) \leq B$  for all policies  $\pi$ .

*Proof.* To prove boundedness of  $g$ , we observe that for all  $t$ :

$$\begin{aligned} \mathbb{E}_\pi |g(s_t, s_{t+1})| &= \mathbb{E}_\pi |c(s_{t+1}) - c(s_t)| \\ &\stackrel{(i)}{=} \mathbb{E}_{(s_t, a_t) \sim \pi} \mathbb{E}_{s_{t+1} \sim \mathcal{P}(\cdot | s_t, a_t)} |c(s_{t+1}) - c(s_t)| \\ &\stackrel{(ii)}{\leq} \mathbb{E}_{(s_t, a_t) \sim \pi} B \\ &= B, \end{aligned}$$

where in step (i) we use the law of iterated expectation and denote by  $\mathbb{E}_{s_t \sim \pi}$  the expectation w.r.t.  $(s_t, a_t)$  generated by following the policy  $\pi$ , and in step (ii) we use Assumption 2.

It follows that

$$\begin{aligned} \mathbb{E}_\pi c(s_T) &= c(s_0) + \sum_{t=0}^{T-1} \mathbb{E}_\pi [c(s_{t+1}) - c(s_t)] \\ &\leq c(s_0) + \sum_{t=0}^{T-1} \mathbb{E}_\pi |g(s_t, s_{t+1})| \\ &\leq c(s_0) + BT, \end{aligned}$$

whence

$$\begin{aligned} J^S(\pi) &= \lim_{T \rightarrow \infty} \frac{1}{T} \mathbb{E}_{\pi, s_0} c(s_T) \\ &\leq \lim_{T \rightarrow \infty} \frac{1}{T} (c(s_0) + BT) \leq B. \end{aligned}$$

□

**Proposition 1.** (Policy gradient of  $J^S$ ) Consider a policy class  $\{\pi_\theta\}$  smoothly parameterized by  $\theta$ . Under Assumptions 1 and 2, for any  $\theta$ , the policy gradient is well-defined and admits the expression

$$\frac{d}{d\theta} J^S(\pi_\theta) = \mathbb{E}_\pi [Q_{\mathcal{M}^S}^{\pi_\theta}((s_{t-1}, s_t), a_t) \nabla_\theta \log \pi_\theta(a_t | s_t)].$$

*Proof.* The claim follows from applying the average-cost Policy Gradient Theorem [48, Theorem 1] to the MDP  $\mathcal{M}^S$  with  $g$  as the cost function, and using the well-known identity  $\pi_\theta(a|s) \cdot \nabla_\theta \log \pi_\theta(a|s) = \nabla_\theta \pi_\theta(a|s)$ . □

**Proposition 2.** ( $J^S$  and rate stability) Under Assumptions 1–3,  $\min_\pi J^S(\pi) = 0$ . Moreover, the system is rate-stable in mean under  $\bar{\pi}$  if and only if  $\bar{\pi} \in \arg \min_\pi J^S(\pi)$ .

*Proof.* By Assumption 1, there exists a stable policy  $\pi_0$  such that  $\mathbb{E}_{\pi_0} c(s_t) < C, \forall t$  for some constant  $C < \infty$ . Therefore,

$$0 \leq \min_{\pi} J^S(\pi) \leq J^S(\pi_0) = \lim_{T \rightarrow \infty} \frac{1}{T} \mathbb{E}_{\pi_0} c(s_T) \leq \lim_{T \rightarrow \infty} \frac{1}{T} \cdot C = 0,$$

hence  $\min_{\pi} J^S(\pi) = J^S(\pi_0) = 0$ .

Consequently, we have  $\bar{\pi} \in \arg \min_{\pi} J^S(\pi)$  if and only if  $J^S(\bar{\pi}) = 0$ . This is in turn equivalent to

$$0 = J^S(\bar{\pi}) = \lim_{T \rightarrow \infty} \frac{1}{T} \mathbb{E}_{\bar{\pi}} c(s_T) = \lim_{T \rightarrow \infty} \frac{1}{T} \mathbb{E}_{\bar{\pi}} c(s_T),$$

which is the definition of rate stability in mean.  $\square$

## B Supporting Content and Empirical Results

In this section, we include additional details and experiments that complement the main results. We also include the code in the supplementary zip file.

### B.1 Visualizations of State Transformations

To provide better intuition of the different state transformations we considered in Section 4.3, we visualize them in Figure 4.

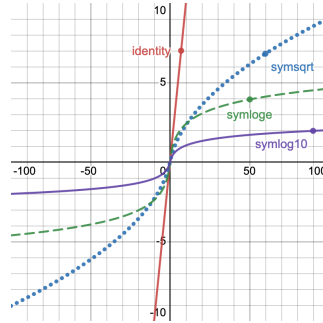


Figure 5: Visualizations of transformation functions.

### B.2 Environments

In this section, we provide additional details about the server allocation and traffic control environment.

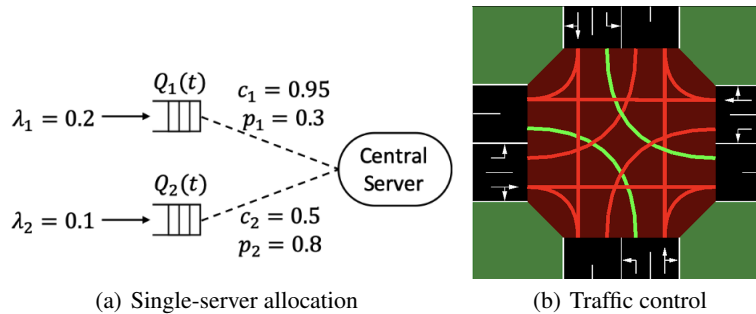


Figure 6: Left: Server-allocation. Image taken from [30]. Right: An example intersection of the traffic control environment. Image taken from [3].

**Single-server allocation queueing** In this environment, there is a single central server that must select among a set of queues to serve. In general, there can be up to  $N$  queues (Figure 6 show a sample 2 queue setup). At each time-step, new jobs arrive in each queue following a Bernoulli process with probability  $\lambda_i$  for queue  $i$ . Note that at each time-step, at most one job enters each queue, which means more than one job may enter the whole system in total. At each time-step, the server must select among the  $N$  queues to serve. A successfully served queue will mean a job will exit that queue, so at most one job can exit the system at a given time-step. When a server selects a queue  $i$ , the server succeeds in making a job exit only if: it can connect to queue  $i$  (which is dependent on the connectivity probability,  $c_i$ ) and the job is successfully served (which is dependent on the service probability,  $p_i$ ). The state of the server is queue length of each queue and 0/1 flag indicating whether the server can connect to a specific queue, resulting in  $2N$ -dimensional state. The action space is index of the queue, resulting in  $N$  dimensions. The goal is to minimize the average queue length. In the non-faulty connection setting, all the connectivity flags are 1. The optimal policy in the faulty connection setting is an open problem [21].

The Bernoulli probability parameters of the tested environments are:

1. 2-queue with faulty connections
  - Arrival rates:  $\lambda_1 = 0.2, \lambda_2 = 0.1$
  - Service rates:  $p_1 = 0.3, p_2 = 0.8$
  - Connection probabilities:  $c_1 = 0.7, c_2 = 0.5$
2. 10-queue with non-faulty connections
  - Arrival rates:  $\lambda_1 = 0.05, \lambda_2 = 0.01, \lambda_3 = 0.2, \lambda_4 = 0.4, \lambda_5 = 0.05, \lambda_6 = 0.01, \lambda_7 = 0.02, \lambda_8 = 0.01, \lambda_9 = 0.015, \lambda_{10} = 0.01$
  - Service rates:  $p_1 = 0.9, p_2 = 0.85, p_3 = 0.95, p_4 = 0.75, p_5 = 0.9, p_6 = 0.9, p_7 = 0.85, p_8 = 0.9, p_9 = 0.9, p_{10} = 0.85$
  - Connection probabilities:  $c_i = 1$  for all  $1 \leq i \leq 10$

**Traffic control** In this environment, a traffic controller must select from a set of phases (shown in green in Figure 6), a set of non-conflicting lanes, to allow cars to move. At each time-step, new cars arrive in each lane at different rates, which determines the traffic congestion level. In our experiments, we considered medium to very high levels of traffic congestion. The state is the number of cars waiting in each lane along with indicator flags for which lanes have a green and yellow light. The action space is the number of phases. The state space is 21 dimensions and the action space is 4. The goal is to minimize the total waiting time of all the cars. To model a real-life traffic situation, the SUMO simulator places a cap of  $\approx 100$  on each lane.

For exact traffic demands used in the experiments, see the `sumo/nets/big-intersection/generator.py` file in the attached code.

### B.3 Additional Empirical Setup Details

**PPO and TPPO Training** We train average-reward PPO and TRPO [59] using the default hyperparameters (network architecture, learning rate, mini batches, epochs over the dataset etc.) in the stablebaselines code base [40]. For all algorithms and variations, we fix the time interval between policy updates during the interaction to be 512 time-steps. For STOP, we hyperparameter sweep only over  $\beta = \{1e^{-4}, 1e^{-5}, 1e^{-6}\}$  and  $\tau_{\text{warmup}} = \{10^6, 2 \cdot 10^6, 3 \cdot 10^6\}$ .

**DQN Training** For the DQN experiments in this supplementary section (see Figure 8), we used the same hyperparameters as above. For average-reward DQN-specific hyperparameters, we set the following: 1) random exploration occurred at a probability of 0.05 and was linearly annealed with time (default is 0.1), 2) exploration and exploitation started from the very beginning of the interaction process (opposed to allowing the agent to explore only for a fixed amount of time before allowing it to exploit), 3) gradient steps to 10, and 4)  $\eta = 1e^{-2}$  (see Eqn 4 in [51]).

Whenever we perform a hyperparameter sweep, we select the agent that achieves the lowest performance metric value at the end of the experiment (Manhattan distance for gridworld, average queue length for queueing, and total waiting time for traffic control).



### B.4 Additional Ablation: Varying $\beta$

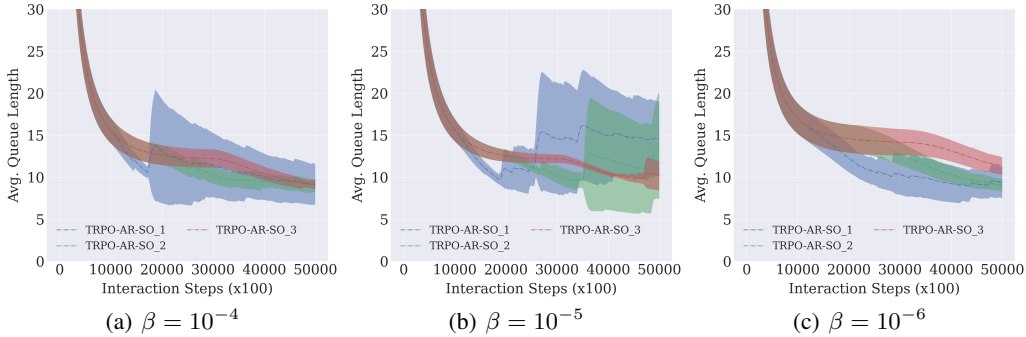
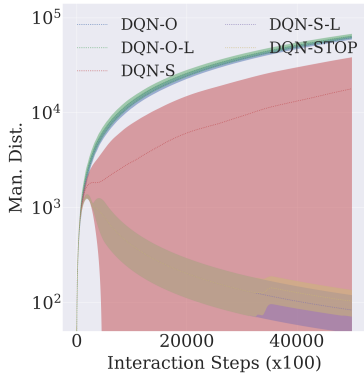


Figure 7: Average queue length vs. interaction time-steps on the 10-queue network for different values of  $\beta$  when applying STOP to TRPO. The legend is read as TRPO-AR-SO- $\langle\tau_{\text{warmup}}\rangle$  in million time-steps. For example, for TRPO-AR-SO-2,  $\tau_{\text{warmup}} = 2 \cdot 10^6$  steps. Performance metrics are computed over 5 trials with 95% confidence intervals. Lower is better.

In section 5, we showed the impact of varying the  $\tau_{\text{warmup}}$  of STOP. In this experiment, we vary  $\beta$ , the speed at which optimality is introduced into the learning process of STOP. We find that slowly introducing optimality (smaller  $\beta$ ) in the learning process is better for achieving lower true cost. For faster rates, we see that the agent starts to make mistakes and has to adapt. This finding also aligns with our earlier conclusion that it is better for the agent to first learn how to be stable before trying to be optimal.

### B.5 STOP + DQN



(a) DQN variations of infinite gridworld

Figure 8: Manhattan distance vs. interaction time-steps on the infinite gridworld when applying STOP to DQN. DQN-O optimizes the optimality criterion only and uses the identity state transformation. DQN-O-L optimizes the optimality criterion but applies symloge to the state. DQN-S optimizes the stability criterion only and uses the identity state transformation. DQN-S-L optimizes the stability criterion only but with applying symloge state transformation. DQN-STOP is all the components of STOP applied to DQN. Performance metrics are computed over 5 trials with 95% confidence intervals. Lower is better. Vertical axis is log-scaled.

In Section 5, we focused on PPO and TRPO due to their widespread use and robustness. Given that STOP is algorithm-agnostic, we apply it to average-reward DQN [51] on the infinite gridworld domain (Figure 8). The state transformation is applied only to the state before it is fed into the action-value function; the reward function is computed based on the original state.

We find that STOP also significantly improves the robustness of DQN. However, optimizing for stability only (and applying symloge on the state) outperforms STOP + DQN, which includes optimality as well. While this result is positive in that it shows the importance of the stability reward *and* the state transformation, it is interesting that the stability-only version of STOP outperforms the general

STOP, which was not the case for TRPO and PPO. We suspect that the non-stationary nature of the reward function (due to reverse annealing) results in the single action-value to chase a moving target, potentially confusing the agent. We hypothesize that decomposing the single action-value into two action-values [41]: a stability action-value and optimality action-value, and then combining the two separate action-values with the reverse annealing approach may mitigate this confusion

More generally, we also find that it is more challenging to train performant policies with DQN in this setting compared to PPO and TRPO, especially when the environment dynamics are highly stochastic. We attribute this finding to the explore-exploit tension. In the continuing task with unbounded state space and high stochasticity, it can be very expensive to explore since poor exploration can lead to divergence. However, exploration is critical for DQN to learn the optimal action-values. Thus, this tension raises an interesting question for future work: how should algorithms such as DQN effectively explore in continuing task with unbounded state spaces and high stochasticity?

## **B.6 Hardware For Experiments**

For all experiments, we used the following compute infrastructure:

- Distributed cluster on HTCondor framework
- Intel(R) Xeon(R) CPU E5-2470 0 @ 2.30GHz
- RAM: 5GB
- Disk space: 5GB